

Photon–ion collisions and molecular clocks

T. OSIPOV[†], A. S. ALNASER[†], S. VOSS[†], M. H. PRIOR[‡],
T. WEBER[§], O. JAGUTZKI[§], L. SCHMIDT[§],
H. SCHMIDT-BÖCKING[§], R. DÖRNER[§], A. LANDERS[¶],
E. WELLS^{||}, B. SHAN[†], C. MAHARJAN[†], B. ULRICH[†],
P. RANITOVIC[†], X. M. TONG[†], C. D. LIN[†] and C. L. COCKE[†]

[†]J. R. Macdonald Laboratory, Physics Department, Kansas State
University, Manhattan, KS 66506, USA

[‡]Lawrence Berkeley National Laboratory, Berkeley, CA, 94720, USA

[§]Institut für Kernphysik, University Frankfurt,
August-Euler-Str. 6, 60486, Frankfurt, Germany

[¶]Physics Department, Auburn University, Auburn, AL, 36849, USA

^{||}Department of Physics, Augustana College, Sioux Falls,
South Dakota, 57197, USA

(Received 22 April 2004; revision received 13 August 2004)

Abstract. The timing of molecular rearrangements can be followed in the time domain on a femtosecond scale by using momentum imaging techniques. Three examples are discussed in this paper: first, the diffraction of electrons ejected from the K-shell of one of the atomic constituents of the molecule takes a ‘picture’ of the molecule, and the correlation between the momentum vector of the photoelectron and the subsequent fragmentation pattern is used to estimate the time delay which accompanies the latter process. Second, the kinetic energy release of proton pairs from the double ionization of hydrogen by fast laser pulses is timed using the optical cycle as a clock. The mechanisms of rescattering, sequential and enhanced ionization are clearly identified in the momentum spectra. Third, the operation of rescattering double ionization in the case of nitrogen and oxygen molecules is discussed.

1. Introduction

Recoil ion momentum imaging, known cryptically as COLTRIMS (cold target recoil ion momentum spectroscopy), has been widely used for many years now in the ion–atom collisions community [1–3]. It has also become a common tool for studying charged particles ejected from atomic and molecular targets by single (synchrotron radiation) photons and intense laser pulses [4–6]. Because the approach provides a comprehensive coverage of the whole ‘charged’ phase space including both electrons and ions, correlations of the momentum vectors are easy to establish with high efficiency. In this article we will summarize two ways in which this approach can be used to provide information on the time evolution of the heavy particle motion when the target is a molecule and ultimately fragments into charged pieces. Both approaches discussed here require the ultimate production of two charged fragments from the molecule. Both approaches use the initial ionization of the molecule to start a clock, and the observation of the energy and

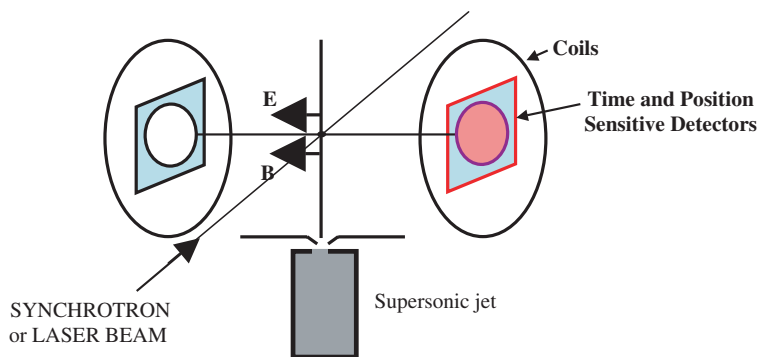


Figure 1. COLTRIMS schematic.

angular emission pattern of the fragments gives information on the explosion pattern. The first example uses hard, deep ionization of the K-shell of one of the molecular constituents and the diffraction of the photoelectron to ‘align’ the molecule. The second, involving short laser pulses, also starts the clock with the emission of the first electron and reads the clock at multiples of the optical period later. The time information is deduced from an analysis, including quantitative modelling, of the final fragmentation patterns after a second electron is also removed.

2. Experiment: momentum imaging

The basic experimental arrangement has been discussed in numerous papers [1–6]. The idea is shown schematically in figure 1. Photons interact with a gas jet target, resulting in the ejection of electron and ions. A uniform electric field projects these oppositely charged particles onto the faces of channel plate detectors. Each detector is equipped with a position-sensitive anode. The times and positions of the hits on the detector are registered by a multi-hit-capable time-to-digital converter and recorded on an event-by-event basis for off-line sorting. Because the electrons are typically more energetic than the ions, a uniform magnetic field parallel to the electric field is also used to keep the electrons from flying transversely off the detector. The momentum vectors of all associated particles are calculated for each event, and the correlations among these momenta are analysed to extract whatever information is desired. The target is a cold gas jet, cooled transversely by tight collimation and along the jet direction by expansion. A supersonic jet is not necessary for the present experiments.

3. Diffraction patterns from ethylene and acetylene: timing the isomerization

We used 300–350 eV photons from the Advanced Light Source at Berkeley to eject photoelectrons with energies of tens of electron-volts from the K-shell of one of the carbon atoms in ethylene and acetylene. When the K-shell electron is removed, the molecule responds by Auger decaying to a doubly charged molecule, thereby populating a variety of electronic states of the dication. The molecule then usually fragments. We see many fragmentation channels in our spectra, but focus

our attention on those which produce two nearly equal-mass singly charged heavy fragments with no neutral atoms missing. That is, for ethylene we look at the $\text{CH}_2^+-\text{CH}_2^+$ channel and for acetylene we look at the CH^+-CH^+ and CH_2^+-C^+ channels. Because the photoelectron leaves the molecule on a time scale of 10^{-17} s, the diffraction pattern is characteristic of the ‘fixed in space’ target molecule. The Auger decay and fragmentation, which last typically tens of femtoseconds or more, occur later. If the fragmentation is not ‘delayed’ but proceeds along a fully repulsive potential curve, the fragmentation time is so fast that rotation cannot occur and the direction along which the two singly charged ions retreat from each other is that of the initial alignment of the molecule. Thus the molecule is fixed in space experimentally *a posteriori*.

Figure 2 shows the resulting photoelectron angular distributions for the case of the ethylene target for three incident photon energies. The data set covers all angles of the molecule relative to the polarization vector, but we show here only spectra for which the molecule is initially aligned along the polarization. It is well known in such molecules as N_2 and CO that a strong f-wave sigma resonance occurs for electrons about 10 to 15 eV above the K-shell ionization threshold [5, 7]. A strong f-wave structure for ethylene is also evident in these spectra, although not as strong for this molecule as for the diatomics. Above and below the ‘resonant’ region, this structure persists, but is weaker. For the case of ethylene, the kinetic energy release (KER) is very sharply peaked with a value near 5 eV, indicating that probably a single electronic energy surface delivers the ions into this fragmentation channel. This behaviour is shown in the lower panel of figure 3, as an xz slice of the relative momentum of the CH_2^+ ion pairs. Here the collection electric field

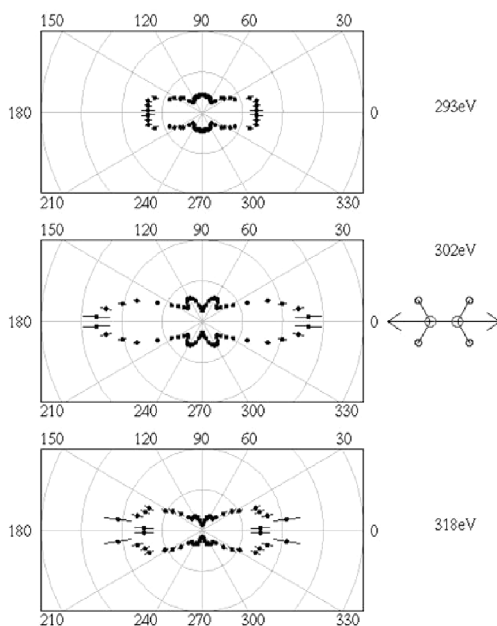


Figure 2. Ethylene photoelectron spectrum, for the case where the target molecule is aligned along the direction of the polarization vector. Three photon energies are shown, below, on and above the ‘resonant’ energy for which the f-wave amplitude maximizes.

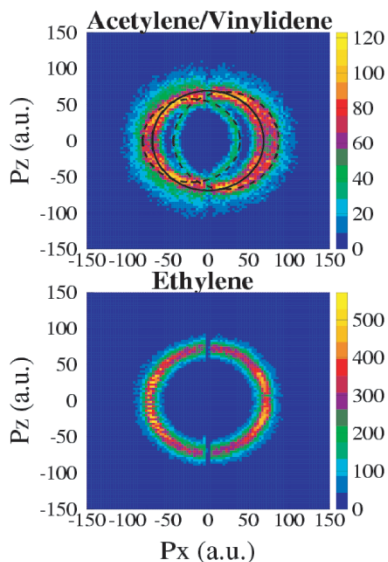


Figure 3. Momentum slices of the ‘explosion’ spheres for the breakup of ethylene (upper panel) and acetylene (lower panel) targets induced by 310 eV photons. The polarization vector (x) is horizontal and in the plane of the page. The photon is moving in the z direction. This figure is from the work by Osipov and co-workers [6].

and photon polarization vectors are along the x axis, the jet along the y axis and the photon propagation direction along the z axis. The figure is made by requiring a relative momentum not exceeding 10 au (au of momentum = \hbar/a_0 , where \hbar is the Planck constant and a_0 is the Bohr radius) in the z direction.

When the ethylene target is replaced by acetylene, a surprise results: the corresponding momentum slice becomes unexpectedly complex and asymmetric. This feature results from the presence in the data of both the acetylene-like CH^+-CH^+ and vinylidene-like C^+-CH_2^+ decay modes. The separation of these channels is somewhat problematic, but possible once the source of the strange patterns are understood. The strange plot of figure 3 results from an evaluation of the data under the assumption that only CH^+ ions are present. This assumption is incorrect. The details of the separation of the acetylene and vinylidene channels, as well as an earlier account of this experiment, are described in [6].

The timing information emerges from the observation that the nice f-wave-like pattern seen for ethylene is still seen when the acetylene target is used, but only when the molecular axis is established using data corresponding to the CH^+-CH^+ decay channel. When the C^+-CH_2^+ channel is used instead, the pattern is washed out. Since the original diffraction pattern is established long before the breakup occurs, this washing out must be due to the method of establishing the molecular axis. It could be due to a time delay between the emission of the photoelectron and the breakup, which could allow the molecular C=C bond angle to rotate slightly before breakup and invalidate the axial breakup assumption. An infinite rotation time would allow the correlation between photoelectron and breakup axes to be lost entirely. The molecule has rotational angular momentum from two sources, the finite gas temperature and the emission of the energetic K Auger electron from one of the carbon atoms. Neither is well known in this, but from the latter

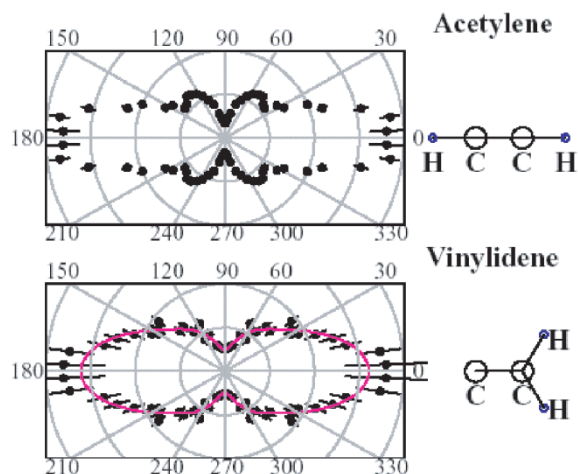


Figure 4. Body-fixed photoelectron angular distributions obtained by fixing the molecule using the acetylene (upper panel) and vinylidene (lower channel) for the case where the molecule is finally within 45° of the x axis. The solid line in the lower panel is the result of the analysis described in the text.

source an angular momentum of approximately $3\hbar$ is expected and the rotational temperature is not expected to yield a higher value.

A rotation angle was extracted from the data using the following procedure: the acetylene data was reanalysed event by event, but before plotting the axis of the molecule, deduced from the ion momentum, was re-directed by a randomly chosen angle with an average value of θ_0 (Gaussianly distributed with a 25% FWHM (full width at half maximum)); the results are very insensitive to the details of the distribution). The parameter θ_0 was then varied so as to reproduce the experimentally observed photoelectron angular distribution obtained using data corresponding to decay through the vinylidene channel. The results are shown in figure 4. The best fit was obtained for a value of θ_0 of 20° . This angle is almost exactly what one would expect for an instantaneous rearrangement whereby the hydrogen atom initially at one end of the molecule proceeds tangentially at constant radius to the other end of the molecule. Such a rotation inevitably accompanies the mass rearrangement, no matter how quick the isomerization. Thus the most important aspect of the observed photoelectron angular distribution as measured using the vinylidene channel is that it is not completely washed out. A great deal of correlation between photoelectron and decay axes is still retained by the molecule even when it decays through the vinylidene channel. By using a more detailed analysis, an upper limit of approximately 100 fs was placed on the isomerization time from acetylene to vinylidene for the particular energy surface followed in this direction of acetylene [7]. This surface is not identified in the experiment, but it is likely to be nearly unique, since the KER observed in the vinylidene channel is nearly single valued at 4.5 eV. The actual decay path for the isomerization process, which was observed much earlier by Thissen *et al.* [8], has been calculated and discussed by Dufflot *et al.* [9].

It is possible that by performing pump-probe experiments with acetylene using femtosecond laser pulses, one could even follow the hydrogen migration in real time. An initial experiment in this direction for acetonitrile has been reported

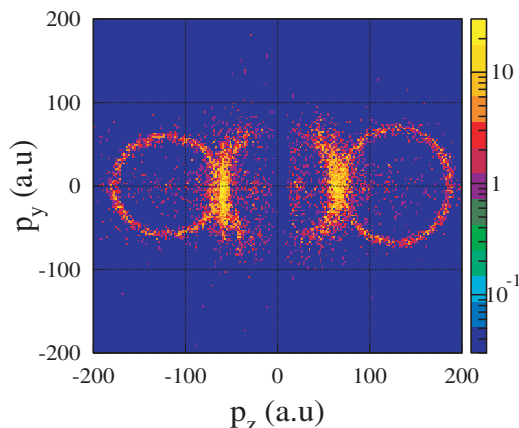


Figure 5. Similar to figure 3, except that now the acetylene is dissociated by a 35 fs pulse of peak power $2 \times 10^{14} \text{ W cm}^{-2}$ and with different extraction field parameters. The outer rings are due to the vinylidene dissociation channel and the inner one to the acetylene channel.

by Hishikawa *et al.* [10]. Figure 5 shows a similar result for the acetylene/vinylidene case. The approach is similar to that discussed above except that only ions are now detected and parameters are chosen which allow an easier separation of the two channels. Pulses of $2 \times 10^{14} \text{ W cm}^{-2}$ and 35 fs duration were used to cause the ultimate fragmentation of the dication of acetylene into the two channels discussed above. Now the rotation information is deduced from the angular distribution relative to the polarization vector rather than with respect to the photoelectron emission angle. It is clear immediately that the acetylene ions are much more strongly peaked along the polarization vector than the vinylidene ions, suggesting a finite delay has intervened between the injection of electronic energy into the molecule by the laser and the breakup for the latter case. This experiment and interpretation are still in progress.

4. Sequencing emission of ion pairs in molecular hydrogen

The double ionization of molecular hydrogen through enhanced ionization is well documented in the literature and heavily studied theoretically [11–14]. In recent years two additional double ionization processes have been identified and modelled: rescattering ionization [15–21] and sequential ionization [22, 23]. Figure 6 shows a schematic of these three processes, roughly ordered according to the intensity region in which each is expected to dominate. These processes all operate on different time scales. The emission of the first electron starts a ‘clock’ and simultaneously launches a wave packet into the $1\sigma_u$ potential of the H_2^+ molecule, where it tries to oscillate with a period of 15 fs. This wave packet runs into trouble before it completes a single cycle. The rescattering process, whereby the electron released in ionization of the neutral returns to the singly charged ion to excite or ionize it further, can occur $2/3$ of an optical period after the first ionization event, and thereafter at full additional optical cycles later (times of 1.8, 4.5, 7.2 fs, etc.). If only the energies of single high energy protons (energies above about 3 eV per proton) are measured, the conclusion is that the first return

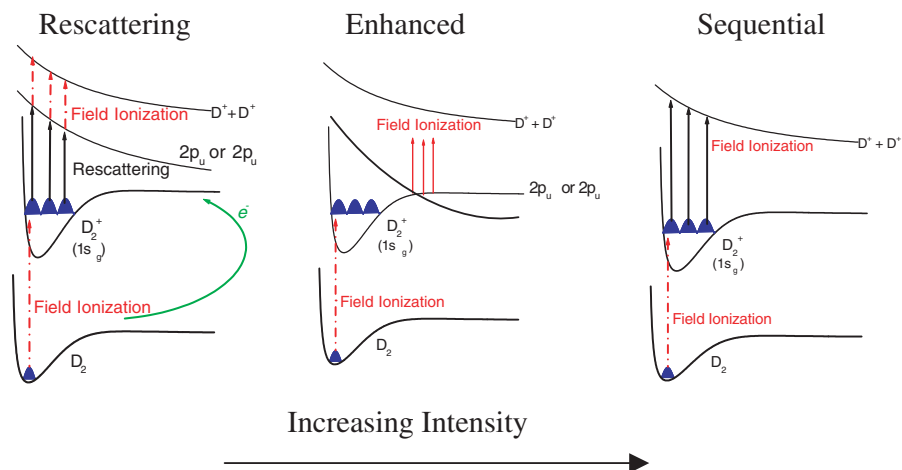


Figure 6. Schematic of three mechanisms for ionization of D_2 (or H_2) by intense laser pulses.

dominates [15, 16]. When the double ionization channel is observed, structure is seen up through the third return and perhaps further [18, 19]. By the time 7.2 fs is reached, the vibrational wave packet launched in the $1\sigma_u$ potential of the H_2^+ molecule has reached its outer turning point and identification of later returns is nearly impossible. When a short pulse, 8 fs, is used however, the first return dominates the rescattering process and high energy protons released from just slightly beyond the equilibrium distance of the neutral molecule are observed. The ‘clock’ starts ticking when the first electron is released, at whichever optical cycle maximum this occurs, and the first double ionization ‘burst’ is released at about 1.8 fs later, so timing with femtosecond precision does not require a femtosecond long pulse. If the vibrational wave packet survives this event, (the rescattering double ionization occurs with a probability which peaks at about 3%) and the field envelope rises fast enough, the second ionization may occur sequentially [22] giving rise to further ionization on the next optical maximum. Model calculations by [22] and by Tong and Lin [23, 24] suggest that the sequential ionization occurs partially over the two optical cycles following the first release, corresponding to ticks of the clock at 2.7 and 5.4 fs after the first ionization. This results in a KER somewhere between that characterizing the internuclear distance of the neutral molecule and that of the outer turning point. Finally, if the wave packet survives both of these processes and furthermore escapes the $1\sigma_u$ potential well, via bond softening for example [25], it passes through the region of enhanced ionization, calculated to occur near 8–10 au [13] and observed near 5 au.

In figure 7 we show a slice of the momentum sphere of Coulomb exploding proton pairs released from molecular hydrogen exposed to 12 fs pulses at $7 \times 10^{14} \text{ W cm}^{-2}$. What is shown is the relative momentum of the two protons, in the molecular frame, sliced through the xz plane. Sequential and enhanced ionization processes are visible in the same spectrum. At this high intensity, rescattering is relatively weak. The relative intensity of the three processes is very sensitive to the laser intensity and pulse length, and a slight change in either will generally result in the domination of the spectrum by one of the three processes. Time in this spectrum proceeds radially inward with $t = 0$, starting when the first

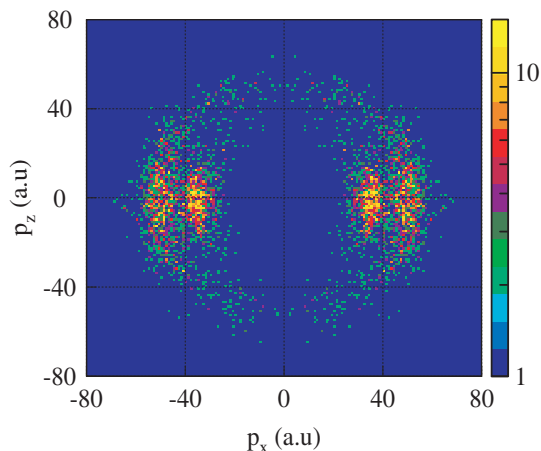


Figure 7. Slice of momenta of exploding proton pairs from ionization of H_2 by 12 fs pulses with a peak intensity of $7 \times 10^{14} \text{ W cm}^{-2}$. The geometry is similar to that of figure 5.

electron is released. Roughly speaking, $t = 0$ corresponds to a radial momentum of 45 au and $t = 7$ fs corresponds to a radial momentum of 20 au. The scale is, of course, not linear and requires a model calculation to interpret it quantitatively. As shown in figure 7 the sequential process is less directional than the enhanced ionization, but it still peaks along the polarization direction. It is not yet fully explained by the model why the sequential ionization is so peaked in angle, since the first ionization step certainly is not. Figure 8 for example shows a comparison between expected and calculated positions of KER for the rescattering and sequential ionization processes. The agreement with the model is excellent. Further discussion of the model is given by Lin *et al.* in a contribution in this same issue [24]. Our ability to distinguish so cleanly all three processes in a single spectrum gives us confidence that these three mechanisms do indeed correspond to real physically distinguishable different processes, each of which can be used to ‘time’ the motion of the wave packet with a clock whose ticks occur as multiples of the optical cycle.

5. Double ionization of heavier molecules

Can the same processes be identified for molecules such as O_2 and N_2 and can one use the same techniques discussed above to follow heavy particle motion in these systems on a very short (< 8 fs) time scale? The same processes almost certainly exist. The enhanced ionization process for these molecules is well known, with the major result being that the KER release observed is much less than that expected from a Coulomb explosion from the internuclear distance of the neutral molecule [26–30]. Non-sequential ionization of these and related molecules has been discussed [31–36], but not clearly characterized, and a similar evaluation applies to sequential ionization. Here we report a few recent results from the observation of only the double ionization channel populated from these molecules by short laser pulses and observed through the dissociative production of singly charged ion pairs $\text{N}^+ - \text{N}^+$ and $\text{O}^+ - \text{O}^+$. In figure 9 we show schematics of processes

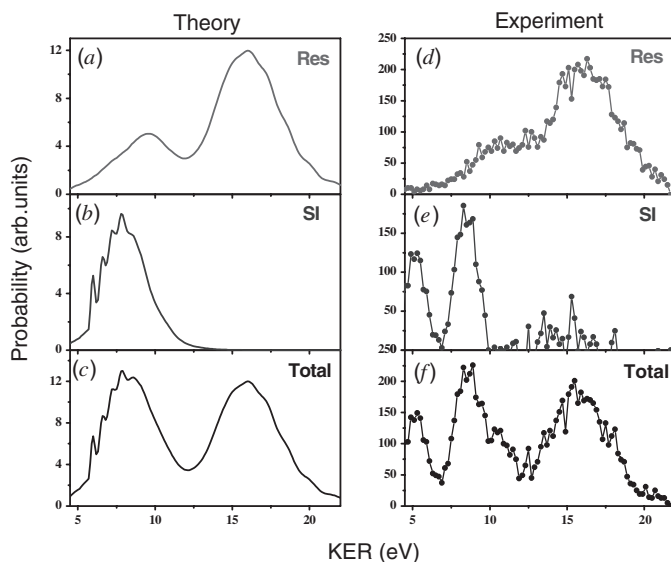


Figure 8. Experimental and theoretical KER spectra for rescattering and sequential processes, deduced from the data of figure 7. The separation of rescattering and sequential KER in the experiment was accomplished using the angular distribution data of figure 7.

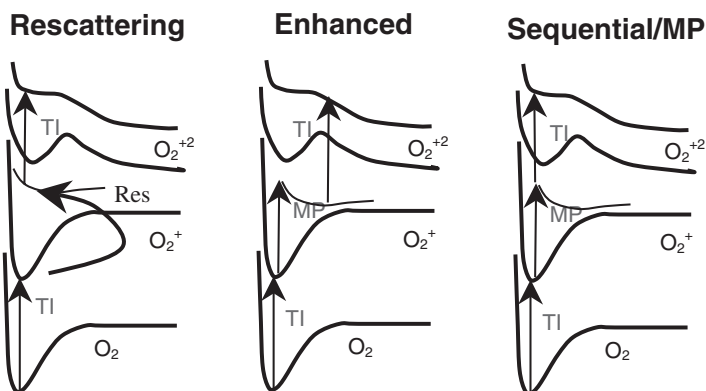


Figure 9. Schematic of possible mechanisms for fragmentation of O_2 , similar to figure 6 (three steps with different ordering may lead to double-ionization; these are tunnelling ionization (TI), multiphoton excitation (MP) or rescattering process (Res)).

analogous to those of figure 6, modified to be appropriate to this case. We note immediately that simply removing the two outer electrons from the molecules in this case will produce a metastable ground state of the molecule which will not dissociate on the time scale of the apparatus. Thus not only does one have to produce a dication, one has to excite it electronically to produce the observed decay mode. Thus the processes of figure 9 differ slightly from those of figure 6. We discuss here only a few recent findings for which we have some explanation.

The first observation is that the usual distinction between non-sequential (rescattering) and sequential ionization intensity regimes holds cleanly for these

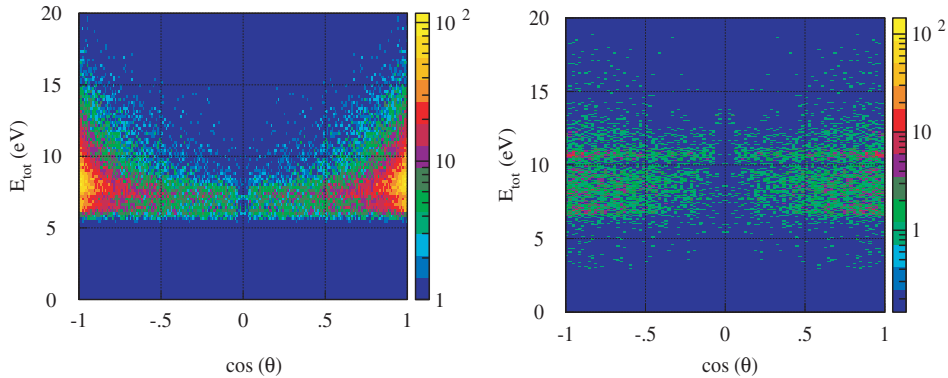


Figure 10. Left-hand panel: a density plot of the yields of coincident $O^+–O^+$ pairs for oxygen targets. The vertical axis is the KER and the horizontal axis is the cosine of the angle between the relative motion of these ions and the polarization vector. Right-hand panel: corresponding plot for nitrogen.

systems. This is established by comparing the ion pair yields with linear and circular polarization (the latter while doubling the power, to maintain the same peak field strength). We observe that below about $2 \times 10^{14} \text{ W cm}^{-2}$ the yield in this channel with circular polarization is nearly negligible, allowing us to establish that data taken at this and slightly lower intensities are in the rescattering regime. This is consistent with the results of [31–36].

Confining our data for the moment to the rescattering region (left-hand panel of figure 9), we find that the fragmentation from both systems proceeds through well-defined states of the dications, as shown in figure 10. This figure shows plots of the KER release as a function of the angle between laser polarization and the molecular axis. The stripes correspond to states in the dication as identified by [37, 38] for electron bombardment of the same targets. For the case of O_2 , these states correspond to electronic configurations of the type $\pi_u^{-1}\pi_g^1$ and $\sigma_u^{-1}\pi_g^{-1}$ where the ‘vacuum state’ is the O_2 neutral. For the case of N_2 , they are $\sigma_g^{-1}\pi_u^{-1}$. Thus the use of the term Coulomb explosion is not really appropriate here: the charge state is too low. One must use real molecular potentials to see the real physics. This result was anticipated in [39]. We believe that the sharpness of the KER in this case is intimately connected to the fact that the rescattering occurs on a very short time scale. We suggest that a process similar to that which occurs for H_2 : a singly charged molecule is produced by removing the outermost $\pi_g(\sigma_g)$ electron for O_2 (N_2), reaching the singly charged cation ground state. The returning electron excites (or possibly ionizes) this molecule and the laser then removes another electron from the same orbital, producing a dissociative excited state of the dication.

The intermediate step must occur quickly enough such that the internuclear distance does not change in order to maintain the KER resolution. We believe the sharp resolution of the KER is associated with the dominance of the first and possibly second return of the electron.

A second feature of these spectra is that the nitrogen ions are emitted only along the laser polarization, while the oxygen ions are emitted over a wider range of angles and even have a slight minimum along the polarization vector. Within the scenario suggested above, this could occur for one of two reasons: first, the single

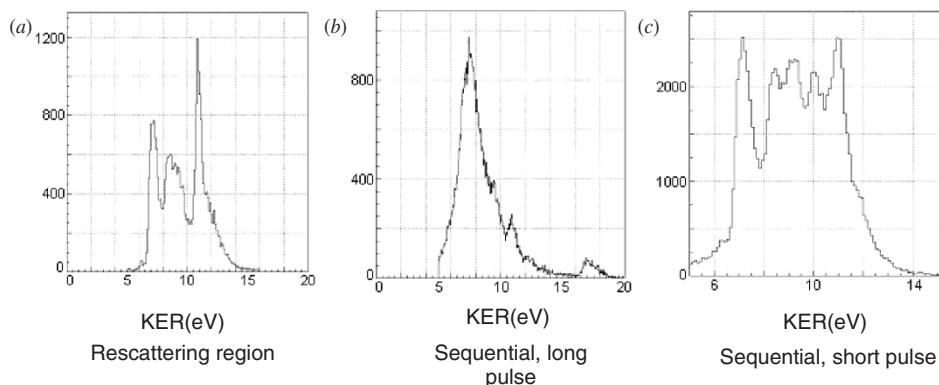


Figure 11. KER spectra for oxygen, for (a) 35 fs pulse, rescattering region, (b) 35 fs pulse, sequential ionization region and (c) 8 fs pulse, sequential ionization region.

ionization of O_2 is expected to preselect molecules aligned at 45° , while for N_2 the corresponding angle is zero degrees. This result is expected from the molecular ADK and from interference models, and has also been seen experimentally for nitrogen by Litvinyuk *et al.* [40]. Second, the returning wave packet emitted along the polarization vector in the oxygen case ‘cancels itself out’ due to the symmetry of the packet, as discussed in [41]. Either would qualitatively explain the observed angular difference seen in figure 10.

If the intensity of the laser is raised into the sequential/enhanced ionization region but the pulse length kept at 35 fs, longer than the oscillation period in the cation potential well, the motion of the internuclear distance between steps can again be seen. The effect is now that the KER spectra are found to ‘wash out’, an effect which is much larger for oxygen than for nitrogen, and which is shown in figure 11. The lowering of the KER is indicative that the ions have time to move radially outward before the second ionizing step occurs. However, if the pulse length is now shortened to 8 fs, denying the wave packet the necessary time to expand before the second step occurs, the KER resolution is regained, as is shown in the third panel of this figure.

Our conclusion at present is that the same systematics observed and quantified for H_2 apply, with some modification, to heavier molecules as well. However, no simple quantitative model has yet been built for the latter case, and such modelling will almost certainly be required before the optical cycle can be used as a reliable clock for timing heavy particle motion in this case.

Acknowledgments

This work was supported by Chemical Sciences, Geosciences and Biosciences Division, Office of Basic Energy Sciences, Office of Science, US Department of Energy. The construction of the laser facility was partially supported by an NSF MRI grant.

References

- [1] DÖRNER, R. D., MERGEL, V., JAGUTZKI, O., SPIELBERGER, L., ULLRICH, J., MOSHAMMER, H., and SCHMIDT-BÖCKING, H., 2000, *Phys. Rep.*, **330**, 95.

- [2] ULLRICH, J., DÖRNER, R. D., MERGEL, V., JAGUTZKI, O., SPIELBERGER, L., and SCHMIDT-BÖCKING, H., 1994, *Comments at. molec. Phys.*, **30**, 285.
- [3] ULLRICH, J., MOSHAMMER, R., DÖRNER, R. D., JAGUTZKI, O., MERGEL, V., SCHMIDT-BÖCKING, H., and SPIELBERGER, L., 1997, *J. Phys. B*, **30**, 2917.
- [4] LANDERS, A., WEBER, TH., ALI, I., CASSIMI, A., HATTASS, M., JAGUTZKI, O., NAUERT, A., OSIPOV, T., STAUDTE, A., PRIOR, M. H., SCHMIDT-BÖCKING, H., COCKE, C. L., and DÖRNER, R., 2001, *Phys. Rev. Lett.*, **87**, 013002.
- [5] WEBER, TH., JAGUTZKI, O., HATTASS, M., STAUDTE, A., NAUERT, A., SCHMIDT, L., PRIOR, M. H., LANDERS, A. L., BRÄUNING-DEMIAN, A., BRÄUNING, H., COCKE, C. L., OSIPOV, T., ALI, I., DIEZ MUINO, R., ROLLES, D., GARCÍA de ABAJO, F. J., FADLEY, C. S., VAN HOVE, M. A., CASSIMI, A., SCHMIDT-BÖCKING, H., and DÖRNER, R., 2001, *J. Phys. B: at. molec. opt. Phys.*, **34**, 3669.
- [6] OSIPOV, T., COCKE, C. L., PRIOR, M. H., LANDERS, A., WEBER, T., JAGUTZKI, O., SCHMIDT, L., SCHMIDT-BÖCKING, H., and DÖRNER, R., 2003, *Phys. Rev. Lett.*, **90**, 233002.
- [7] OSIPOV, T., 2004, PhD Dissertation, Kansas State University, USA (unpublished).
- [8] THISSEN, R., DELWICHE, J., ROBBE, J. M., DUFLLOT, D., FLAMENT, J. P., and ELAND, J. H. D., 1993, *J. chem. Phys.*, **99**, 6590.
- [9] DUFLLOT, D., ROBBE, J. M., and FLAMENT, J. P., 1994, *J. chem. Phys.*, **102**, 355.
- [10] HISHIKAWA, A., HASEGAWA, H., and YAMANOUCHI, K., 2004, *Phys. Scr.*, to be published.
- [11] POSTHUMUS, J. H., FRASINSKI, L. J., GILES, A. J., and CODLING, K., 1995, *J. Phys. B*, **28**, L349.
- [12] SEIDEMAN, T., IVANOV, M. YU., and CORKUM, P. B., 1995, *Phys. Rev. Lett.*, **75**, 2819.
- [13] ZUO, T., and BANDRAUK, A. D., 1995, *Phys. Rev. A*, **52**, R2511.
- [14] BANDRAUK, A. D., 1999, *Comments at. molec. Phys. D*, **1**, 97.
- [15] NIKURA, H., LÉGARÉ, F., HASBANI, R., BANDRAUK, A. D., et al., 2002, *Nature*, **417**, 917.
- [16] NIKURA, H., LÉGARÉ, F., HASBANI, R., IVANOV, M. YU., VILLENEUVE, D. M., and CORKUM, O. B., 2003, *Nature*, **421**, 826.
- [17] STAUDTE, A., COCKE, C. L., PRIOR, M. H., BELKACEM, A., RAY, C., CHONG, H. W., GLOVER, T. E., SCHOENLEIN, R. W., and SAALMANN, U., 2002, *Phys. Rev. A*, **65**, 020703(R).
- [18] ALNASER, A. S., OSIPOV, T., BENIS, E. P., WECH, A., SHAN, B., COCKE, C. L., TONG, X. M., and LIN, C. D., 2003, *Phys. Rev. Lett.*, **91**, 163002.
- [19] TONG, X. M., ZHAO, X., and LIN, C. D., 2003, *Phys. Rev. Lett.*, **91**, 233203.
- [20] TONG, X. M., ZHAO, X., and LIN, C. D., 2003, *Phys. Rev. A*, **68**, 043412.
- [21] SAKAI, H., LARSEN, J. J., WENDT-LARSEN, I., OLESEN, J., CORKUM, P. B., and STAPLEFELD, H., 2003, *Phys. Rev. A*, **67**, 063404.
- [22] LÉGARÉ, F., LITVINIYUK, I. V., DOOLEY, P. W., QUÉRÉ, F., BANDRAUK, A. D., VILLENEUVE, D. M., and CORKUM, P. B., 2003, *Phys. Rev. Lett.*, **91**, 093002.
- [23] TONG, X. M., and LIN, C. D., 2003, *Phys. Rev. A*, **68**, 043412.
- [24] TONG, X. M., ZHAO, Z. X., and LIN, C. D., 2005, *J. mod. Optics*, **52**, 185.
- [25] ZAVRIYEV, A., BUCKSBAUM, P. H., MULLER, H. G., and SCHUMACHER, D. W., 1990, *Phys. Rev. A*, **42**, 5500.
- [26] NIBARGER, J. P., MENON, S. V., and GIBSON, G. N., 2001, *Phys. Rev. A*, **63**, 053406.
- [27] CODLING, K., CORNAGGIA, C., FRASINSKI, L. J., HATHERLY, P. A., MORELLEC, J., and NORMAND, D., 1991, *J. Phys. B*, **24**, L593.
- [28] CORNAGGIA, C., LAVANCIER, J., NORMAND, D., MORELLEC, J., AGOSTINI, P., CHAMBARET, J. P., and ANTONETTI, A., 1991, *Phys. Rev. A*, **44**, 4499.
- [29] POSTHUMUS, J. H., CODLING, K., FRASINSKI, L. J., and THOMPSON, M. R., 1997, *Laser Phys.*, 813.
- [30] GIBSON, B. N., LI, M., GUO, C., and NIBARGER, J. P., 1998, *Phys. Rev. A*, **58**, 4723.
- [31] GUO, C., LI, M., NIBARGER, J. P., and GIBSON, G. N., 2000, *Phys. Rev. A*, **61**, 033413.
- [32] GUO, C., and GIBSON, G. N., 2000, *Phys. Rev. A*, **63**, 040701.
- [33] GUO, C., LI, M., NIBARGER, J. P., and GIBSON, G. N., 1998, *Phys. Rev. A*, **58**, R4271.
- [34] CORNAGGIA, C., and HERING, PH., 1998, *J. Phys. B*, **31**, L503.

- [35] CORNAGGIA, C., and HERING, PH., 2000, *Phys. Rev. A*, **62**, 023403.
- [36] EREMINA, E., LIU, X., ROTTKE, H., SANDNER, W., SCHÄTZEL, M. G., DREISCHUH, A., PAULUS, G. G., WALTHER, H., MOSHAMMER, R., and ULLRICH, J., 2004, *Phys. Rev. Lett.*, **92**, 173001.
- [37] LUNDQVIST, M., EDVARDSSON, D., BALTZER, P., LARSSON, M., and WANNBERG, B., 1996, *J. Phys. B*, **29**, 499.
- [38] LUNDQVIST, M., EDVARDSSON, D., BALTZER, P., and WANNBERG, B., 1996, *J. Phys. B*, **29**, 1489.
- [39] NIBARGER, J. P., MENON, S. V., and GIBSON, G. N., 2001, *Phys. Rev. A*, **63**, 053406.
- [40] LITVINYUK, I. V., LEE, K. F., DOOLEY, P. W., RAYNER, D. M., VILLENEUVE, D. M., and CORKUM, P. B., 2003, *Phys. Rev. Lett.*, **90**, 233003.
- [41] BHARDWAJ, V. R., RAYMER, D. M., VILLENEUVE, D. M., and CORKUM, P. B., 2001, *Phys. Rev. Lett.*, **87**, 253003.